



1

2 A modeling System for Identification of Maize Ideotypes, optimal sowing dates and nitrogen
3 fertilization under climate change – PREPCLIM-v1

4

5

6 Mihaela Caian^(1*), Catalin Lazar⁽²⁾, Petru Neague⁽¹⁾, Antoanela Dobre⁽¹⁾, Vlad Amihaesei⁽¹⁾, Zenaida
7 Chitu⁽¹⁾, Adrian Irasoc⁽¹⁾, Andreea Popescu⁽¹⁾, George Cizmas⁽²⁾

8

9 ¹- Național Meteorological Administration Romania (NAM), Sos. București-Ploiești nr.97, Sector 1,
10 013686 București România

11 ² – National Agricultural Research and Development Institute (NARDI) Fundulea, 915200 Călărași,
12 România

13 * Corresponding author: mihaela.caian@gmail.com

14

15

16 Abstract

17

18 The impact of climate change on crops and agricultural yield is an actual threat while being a
19 challenging issue due to the high complexity of factors that intervene at the local scale of the crop.
20 Assessing it, requires the use of coupled models climate-phenology, meanwhile methods to identify
21 management and genotypes suitable for local future conditions, in order to sustain adaptation strategies.
22 We present the implementation and use of a new integrated climate-phenology adaptation support
23 modeling system based on regional CORDEX climate models and the CERES Maize model from
24 DSSAT platform, with new modules for optimal management and genotype identification using a
25 hybrid method: deterministic modeling and -ML/ genetic algorithms. It was run as a regional pilot over
26 Romania, operating in real-time in interaction with users, performing agro-climate projections
27 (combination of fertilization, sowing date, soil) and providing best crop management simulated under
28 climate change projections. Multi-model ensemble simulations for two climate scenarios RCP4.5 and
29 RCP8.5 and twelve management scenarios show new results for the region.

30 For the actual genotype we find a projected mean decrease in yield in both climate scenarios for all
31 sowing dates and fertilization levels tested, response shown to be sensitive to initial soil parameters.
32 This response was linked to two factors: a shorter growing season by up to 10% and a loss of
33 fertilization efficiency in a warmer climate. A warning points to results showing a narrowing of agro-
34 management opportunities for crop yield but in opposite it is shown a significant role of optimal
35 genotype-range identification that may provide crop solutions under climate change even in extreme
36 years. Identifying best genotype under warmer climate along sets of six cross-parameter simulations
37 show systematic lower values of the maximal yields, but emphasizes genotype windows of increases in
38 the intermediate yield values in scenarios compared to actual climate. The highest harvest sensitivity to
39 genotype is shown to be to changes in the thermal time to juvenil respectively to maturity stage under
40 warmer climate. The results sustain using a deterministic coupled modeling system combined with
41 data-driven modeling for identifying optimal adaptation including fertilization paths that contribute to
42 climate change mitigation.

43

44

45

1

2

3



46

47 1. Introduction

48

49 According to the IPCC reports (IPCC, 2022) climate change is evident and the prospects appear more
50 worrying today than a few decades ago. Although progress is being made in studying the impacts of
51 climate change on crops and agricultural yield (Arnell and Freeman, 2021; Hatfield et al., 2021, these
52 are rarely directly applicable to provide solutions due to the extremely high complexity of factors that
53 intervene at the local scale of the crop (Malhi et al., 2021, Eyring et al., 2021). These factors include
54 culture-scale sensitivities to the interacting climate sub-components atmosphere/ soil/ phenological
55 processes/ ecosystems, to climate change, to natural causes or human activities (Wheeler and Braun,
56 2013, Xie et al., 2023).

57

58 Taking into account scientific research estimating that the world population will continue to grow and
59 it is expected to arrive to 9,1 milliards until the year 2050 (Godfray and Charles, 2010), the total food
60 yield will have to grow by 70-100% (Smil, 2005; World Development Report, 2008; Selvaraju et al.,
61 2011). Meanwhile the agro-climatic conditions are expected to become vulnerable and gradually, more
62 deficient in the context of climate change and its impact on water availability (Villalobos et al., 2012;
63 van Ittersum et al., 2013; Roccuzzo et al., 2014; Stehr and von Storch, 2009).

64 Another face of the problem comes from the need that approaches and solutions should both: merge
65 user needs, and be in line with neutral climate adaptation stringency (Semenov et Stratonovitch, 2015;
66 Dainelli et al., 2022; Mitchell et al., 2022).

67

68 Early studies on climate change impact on crops have pointed to the need of very high resolution
69 modeling, capable of representing management practices and local scale impact of climate on plant as
70 temperature and precipitation (Trnka et al., 2015; Adams et al., 1998; Mkee et al., 1993) affecting water
71 stress (e.g. the stomatal opening, stem water potential, leaf transpiration efficiency (Espadafor et al.,
72 2017)). Further at regional scale, water availability relation to yield indicated a strong dependence on
73 crop, region, time-scale and plant physiological stage (Webber et al., 2020; Webber et al. 2018; Ceglar
74 et al., 2020; Wu et al., 2021; Berti et al. 2019; Marcinkowski and Piniewski 2018). In this regard, under
75 future climate changes, perspectives for corn yield rises (15%) under irrigated conditions were
76 identified by simulations for areas currently more arid than the geographical region of interest
77 considered in this paper (Kothari et al., 2022). This points out the need for continuation of the
78 simulations taking in consideration soil humidity accuracy and various irrigation strategies.

79 Apart from atmospheric conditions, soil changes significantly affect plant growth through interactions
80 with climate and through changes in chemical compositions. Increasing air temperature was shown to
81 affect the soil carbon budget, its decrease affecting plant and root level processes, biochemical cycles,
82 and species (Abhik Patra et al., 2021).

83

84 Modeling at local, regional and also global scale reported significant advances in understanding,
85 simulating and projecting future crop (Tao et al., 2009; Ganguly et al., 2010; Cock et al., 2021; Chen
86 and Tao, 2022; Schauburger et al., 2020). These emphasize global projected yield mean reductions
87 (Asseng et al., 2015) with differences in the regional pattern of climate change impact on crop and
88 yield (Li et al. 2022). Not only projected regional but also time variability of the impact appears larger
89 and accelerated, motivating intensified efforts on seasonal predictions of plant development and yield
90 (Baez-Gonzalez et al., 2005; Jin et al., 2022) using crop models. These simulations' results significance

4

5

6



91 was analyzed suggesting the need to include crop uncertainty in climate scenarios assessments (Meehl
92 *et al.*, 2007, Rosenzweig *et al.*, 2013, Basso Bruno *et al.*, 2019; Chapagain *et al.*, 2022). In addition,
93 model simulations proved to be a highly useful tool in plant breeding analysis (Bernardo, 2002;
94 Hoogenboom *et al.*, 2004; Cooper and Messina *et al.*, 2023) considered a support in developing
95 superior genotypes and plant-breeding methods for maximizing crop effectiveness. Demonstrations of
96 model simulations' potential as a valuable tool for breeders were reported in finding paths for optimal
97 cultivar using techniques such as parental selection, breeding by design, etc. (Peleman and van der
98 Voort, 2003, Qiao *et al.*, 2022).

99 In most recent years developments climate-crop modeling extended from deterministic crop models
100 (Boogaard *et al.* 2013; Morell *et al.*, 2016) to data-driven techniques or hybrid approaches for assessing
101 crop response to weather and climate change (Zhuang, 2024; Morales and Villalobos, 2023, Meroni
102 *et al.*, 2021; Schwalbert *et al.*, 2020; Zhang *et al.*, 2021). Statistical methods as well as ML used for crop
103 forecast and modeling were however shown to bring for now, limited benefits (Paudel *et al.* 2021),
104 pointing to possibly hybrid techniques that include physical process in the modeling as a key approach
105 for this challenging issue.

106 On the other hand, deterministic breeding techniques using model simulations require a huge number
107 of simulations, analysis and inter-comparisons of predicted cross performance (Wang and Pfeiffer,
108 2007).

109

110 Here we present a novel approach developed in the frame of the PREPCLIM (“preparing for Climate
111 Change”) project in which we solve plant phenology development using deterministic modeling and
112 merge this technique with ML-genetic algorithms along simulations in order to iteratively select a
113 cross-range of optimal genotype parameters according to a pre-set user-criteria of the optimum. Genetic
114 algorithms (GA) simulate the evolution of a population by iteratively applying genetic operators, such
115 as selection, crossover, and mutation, to a set of candidate solutions (chromosomes). The chromosomes
116 represent potential solutions to the problem and are encoded as strings of binary or symbolic values,
117 with their fitness assessed by a problem-specific evaluation function here, user-request based. GA was
118 successfully used with DSSAT for optimizing irrigation and fertilizer applications (Bai *et al.*, 2021,
119 Wang *et al.*, 2023).

120

121 The hybrid approach implemented here presents the advantage of physically treating the crop complex
122 process involved each time along optimizing iterations, so allowing analysis of causes of the responses
123 to various climate or /and management scenarios, meanwhile enhancing the ability of choosing
124 optimum conditions from a continuous interval, not a discrete one, of gene parameter values. The
125 continuum values approach is an important feature mainly for isolated extremes, or broad parameters'
126 range, both of increasing interest, as we show in this work the a tendency toward narrower adaptation
127 opportunity windows under warmer climate.

128

129 We present the system developed and data flow in section 2. The motivation of its development, linked
130 to projected climate change in the target region are shown in section 3a. We show results of the system
131 used to estimate changes in plant phenology and crop parameters under climate change scenarios and
132 for different management scenarios, for the actual control genotype in section 3b. Then we discuss in
133 section 3c, results using the genotype optimization package of the system. Perspectives and conclusions
134 are discussed in section 4.

135

7

8

9



136

137

138

139 2. Data and methods

140

141 Projected changes in agro-climate indicators over Romania are computed for two climate scenarios:
142 RCP45 and RCP85 as anomalies reported to historical simulations, using an ensemble of three
143 CORDEX models (Benestad et al., 2021). Then, projected changes in phenological and yield
144 parameters are simulated using the DSSAT crop model (Hoogenboom et al., 2019; Jones et al., 2003)
145 forced with the atmospheric conditions from the CORDEX models (from GFDL, HadGEM, MiROC,
146 IPSL, NorESM), for each model of the ensemble for the historical period and for each of the two
147 climate scenarios.

148 A software package was developed for the DSSAT model that performs identification of optimal
149 model parameters set-up according to user-criteria, user chosen climate-management scenario, region,
150 time-horizon. The user-criteria for optimisation includes maximum yield, stable yield, across years,
151 minimizing the amount of leached nitrogen below the maximum level of the root front (reducing the
152 risk of water pollution), etc. Management scenarios include cross-options for sowing date, fertilization
153 amount, genotype (six parameters defining the genotype). By default, twelve agro-management
154 simulations are performed, for four planting dates (separated by 5 days interval) and three fertilization
155 amounts with Nitrogen (zero, a mean value of the region and the double of the mean value). For each
156 agro-management scenario, genotype optimization by selection of the values for the cultivar related
157 coefficients (named further G-parameters) was performed through two methods: a fixed-discretisation
158 runs and post-processing ordering and a continuum space-search with iterative selection along
159 simulations, by genetic algorithms methods (GA). The proposed GA-based method commences with an
160 initial population of randomly generated chromosomes and undergoes iterative cycles (generations). In
161 each generation, a selection process is performed to choose the fittest chromosomes to reproduce, based
162 on their fitness scores. Subsequently, crossover (recombination) and mutation operators are applied to
163 the selected chromosomes, generating offspring that inherit traits from their parents. The new offspring
164 replace some of the least fit individuals in the population, ensuring that the average fitness of the
165 population improves over time. The convergence of the GA toward an optimal or near-optimal solution
166 is achieved by balancing exploration (searching the problem space for diverse solutions) and
167 exploitation (refining the best solutions found so far). Here GA have even been applied to develop an
168 innovative crop selection algorithm to optimize genotype along agro-management scenarios. Steps
169 along the algorithms are shown in Schema from Annex1.

170

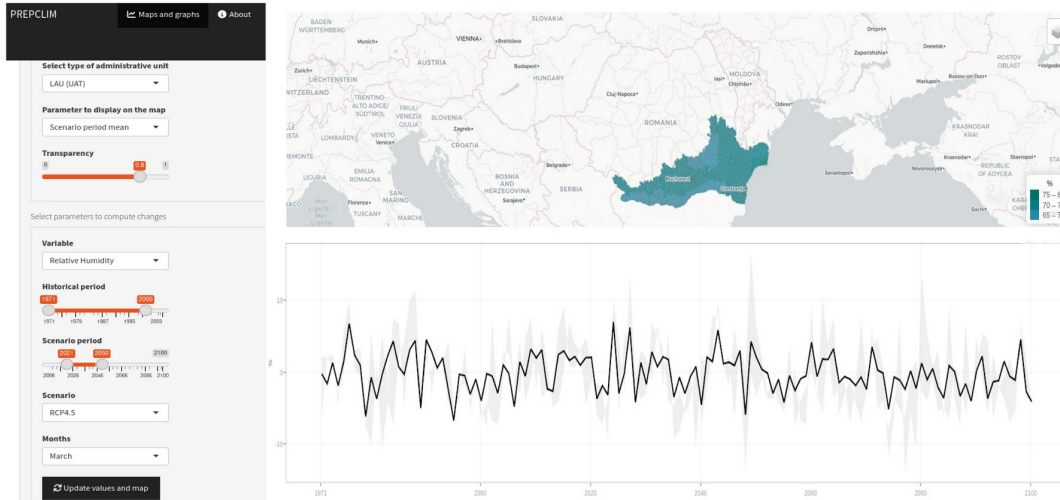
171 The overall output information from the system (climate, agro-climate and optimal paths) is directed on
172 two platform-components (Fig.1). One is a platform (Info-Platform, Fig. 1a) providing static agro-
173 climate information at local scale (NUTS3) over the region, delivering climate indicators, agro-climate,
174 and agro-climate extremes indices computed from observations and re-analysis for the actual climate
175 and from climate scenarios (anomalies relative to historical runs) for future.

176 The second platform is an operational online, user-interactive in real-time component, where requests
177 are placed, treated, and results sent back to the user (User-Platform, Fig. 1b).

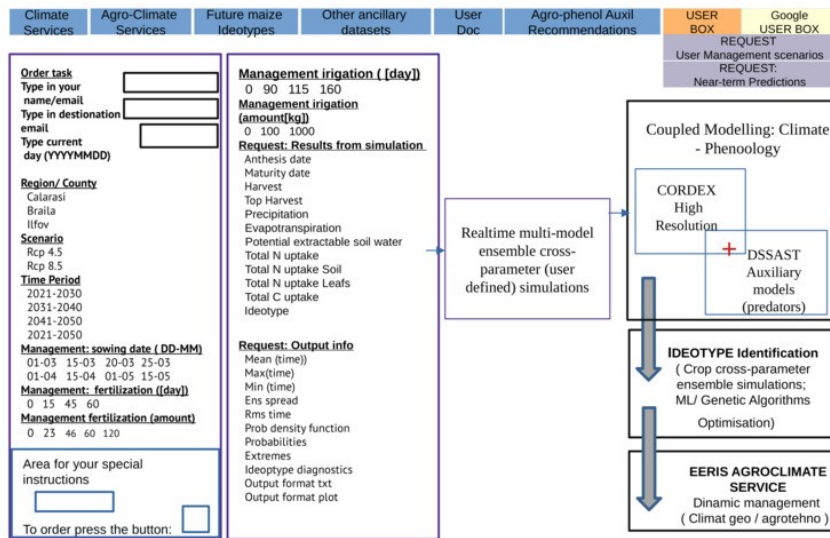
10

11

12



179 Fig. 1a: Info-Platform for information at local scale, derived from regional climate high resolution
 180 models CORDEX, presenting climate, agro-climate, agro-climate extremes indices at NUTS3 level.
 181



182 Fig. 1b: User-Platform: the user-interactive component to specify requests on adaptation management
 183 simulations. User request (left) on: the region, time slice present or climate scenarios, choices for:
 184 sowing date, fertilization/ irrigation (time, amount), genotype and output requests (right) on results:
 185 yields, phenology dates, evapo-transpiration, N and C balance, optimal management path (dates,
 186 management), optimal genotype.

13
 14
 15



187

188 The pilot area where the system was implemented and validated is Southern Romania, for maize. The
189 potential beneficiaries of this system are users, researchers, farmers, and policy makers. Maize breeders
190 also can adapt using the system to the climate conditions by accommodating or testing genotypes that
191 are more resistant to challenging climate. Accelerated climate change makes such a system a useful
192 support in many respects.

193

194 The core of the modeling system relies on coupled modeling by DSSAT crop model (Linux OS)
195 interfaced with regional climate models (Fig.2), with new feature allowing multiple cross-parameter
196 simulations under iterative loops (parameter perturbations) and new features for optimal agro-
197 management x genotype identification (parameter' value selection).

198

199

200

201

202

203

204

205

206

207

208

209

210

211

212

213

214

215

216

217

218

219

220

221

222

223

224

225

226

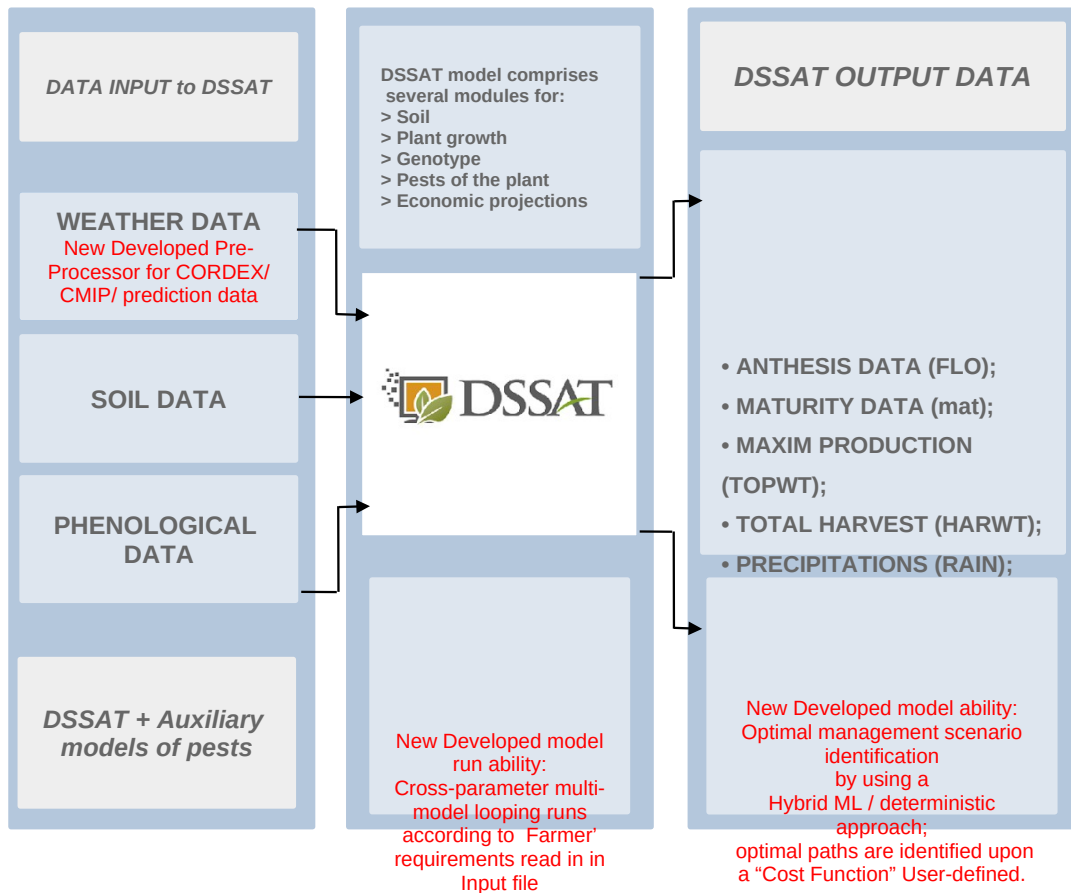
227

228

229

230

231



228 Fig. 2: DSSAT-core and the Optimal-Crop modeling system. Data flow: Input data (left), output
229 information (right); model components and set-up (middle). Red modules were developed within the
230 project.

231

16

17

18



232

233 Table 1: Treatment description in terms of the sowing date and fertilization amount, N [kg/ha].

Treatment	TR1	TR2	TR3	TR4	TR5	TR6	TR7	TR8	TR9	TR10	TR11	TR12
Sowing date	1.04	15.05	1.05	15.05	1.04	15.05	1.05	15.05	1.0	15.05	1.05	15.05
Fertilization (3N)	Fx0=0	Fx1=6	Fx2=1	Fx0=20	Fx1	Fx1	Fx1	Fx1	Fx	Fx2	Fx2	Fx2
Fertilization (1N)	Fx0=0	Fx1=2	Fx2=4	Fx0=6	Fx1	Fx1	Fx1	Fx1	Fx	Fx2	Fx2	Fx2

234

235

236

237

238

239 3. Results

240

241 a) Agro-climate changes in the region

242

243 a.1) Changes in agro-climate indicators

244

245 Agro-climate Indicators (provided on Info-Platform) are computed from CORDEX models, and
 246 provide derived parameters information as time slices for ensemble or model metrics from country to
 247 NUT3 level over South Romania. At the country region Fig.3 shows projected changes in main agro-
 248 climatological characteristics. Region’s climate is expected to shift as shown (Fig. 3a) by the Johansson
 249 continentality index (Baltas, E. 2007; Flocas, 1994) defined as:

250

$$251 JCI = 1.7 \frac{dT}{\sin(\phi)} - 20.4$$

252

253 where dT is the annual maximal thermal range of monthly mean temperatures and ϕ is the latitude.
 254 Changes in JCI show an increase in the entire Southern part up to 5.5% of the interval required to
 255 switch to “extreme continental” from “continental” class already in the first 10 years (2021-2030) in
 256 the ensemble mean (and up to 10% change per model). Changes are towards “maritime” in the
 257 Northern half, this zonal differentiation creating strong thermal wind gradients and being stronger in
 258 RCP85. For agriculture, an often-used regional-indicator is the scorching days number (SC), computed
 259 over the region as the number of degrees in summer days (JJA) over the temperature of 34°C. SC is
 260 constantly increasing (Fig. 3a) in the overall country, with a stronger increase in RCP85 both, in the
 261 first decade and until 2050 than in RCP45, emphasizing as well, the enhancement of the north- south
 262 gradient. Relevant for composed temperature and precipitation, the deMartonne aridity index (IM)
 263 computed as the ratio between annual total precipitation ([mm]) and annual mean temperature ([C
 264 +10) shows in Fig. 3b significant changes in its classes as well, decreasing (towards aridity) mainly in
 265 the South, SE and SW, the main agricultural areas discussed here. Identification of projected changes in
 266 aridity was shown to be a key issue for adaptation in semiarid environments (Ignacio Lorite, et al,
 267 2018).

19

20

21



268 We summarize that changes are accelerating in the South in RCP85 (differences 2071-2100 versus Hist
 269 are higher than those over 2021-2050).

270

271

272

273

274

275

276

277

278

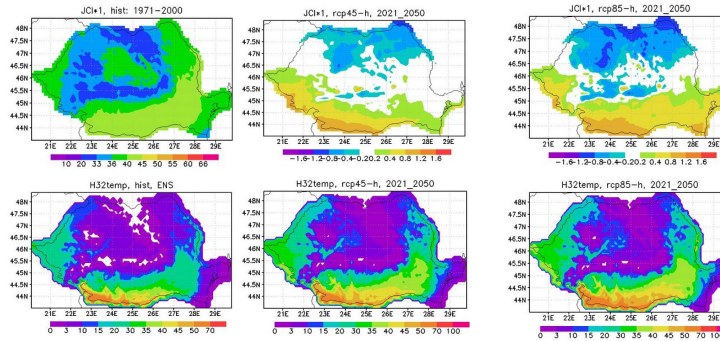
279

280

281

282

283



284 Fig. 3a: Historical (left) and changes relative to it under RCP45 (middle) and RCP85 (right) along
 285 2021-2050, for: the Johansson conventionality index JCI (top): the JCI climate is marine for $0 < k < 33$,
 286 continental for $33 < k < 66$ and exceptionally continental for $67 < k < 100$; the Scorching index SC
 287 (bottom).

288

289

290

291

292

293

294

295

296

297

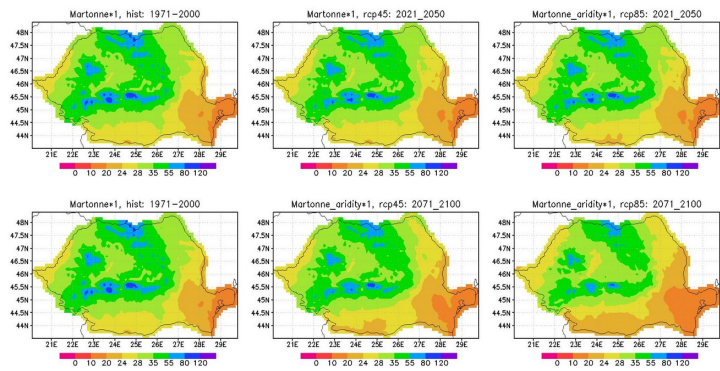
298

299

300

301

302



303 Fig. 3b: Historical (left) and changes relative to it under RCP45 (middle) and RCP85 (right) along
 304 2021-2050 (top) and 2071-2100 (bottom) for the Martonne aridity index. ($0 < IM < 10$ arid; $10 < IM < 20$
 305 semi-arid; $20 < IM < 24$ Mediterranean; $24 < IM < 28$ semi-humid; $28 < IM < 36$ wet; $36 < IM < 55$ very wet;
 306 $ID > 55$ extreme wet).

307

308

309 a.2) Changes in agro-climate extremes

310 Projected changes in extremes are analyzed for the ensemble models in Fig. 4 that shows for Călărași
 311 target subregion changes in RCP85 versus Hist, in the number of freezing days (FD), total precipitation
 312 (RR), severe precipitation (RR10 the number of days with daily accumulated > 10 mm) and total

22

23

24



313 precipitation (RR), for each of the three decades (10 days) of April (the main sowing month for maize).
314 We note a decreasing tendency in FD for both decades, but interestingly intervals with even higher
315 numbers of FD may occur in RCP85 scenario compared to Hist in the third decade. This late spring
316 blizzard feature over the region, important for plant evolution, was shown in a previous work, to be
317 related to the combined context of Polar Jet instability meanwhile with warmer sea surface temperature
318 in the Eastern Mediterranean (Caian and Andrei, 2019). Both these features are projected to enhance in
319 a warmer climate (Lelieveld et al., 2012; Shaw and Miyawaki, 2024;), which for the region indicates a
320 higher potential for severe spring blizzard, affecting crops and the year's yield under warmer climate.

321

322

323

324

325

326

327

328

329

330

331

332

333

334

335

336

337

338

339

340

341

342

343

344

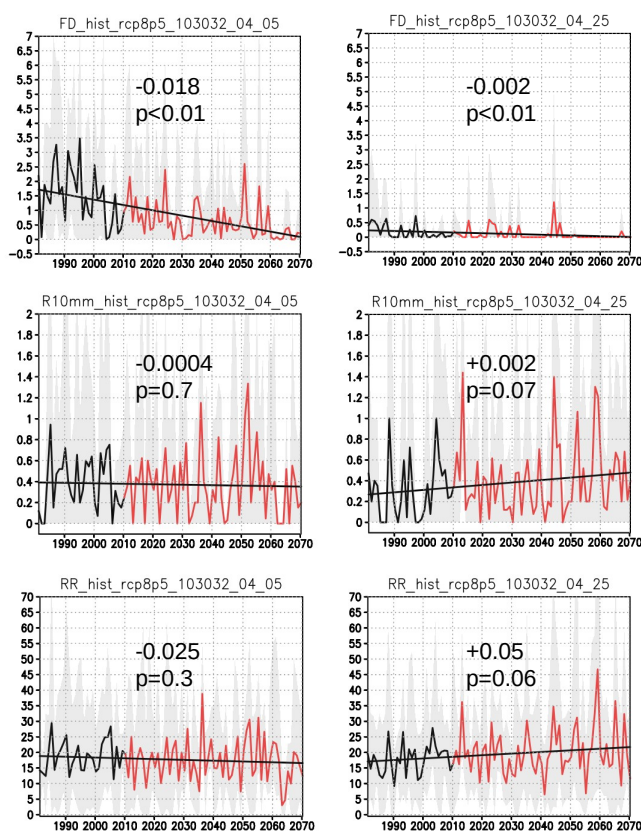
345

346

347

348

349



350

351

352

353

354

355

356

357

Fig. 4: Time evolution ([years], Ox axis) in Hist and RCP85 (1981-2070) of extreme climate parameters: number of frost days (minimum temperature $<0^{\circ}\text{C}$, per 10 days slice, top), number of days total per 10days slice with heavy precipitation ($>10\text{mm}$) (middle); precipitation sum (10 days, [mm] bottom); 10 days slices are centered: 5 April (left), 25 April (right). Boxes indicate the slope of the linear trend (black line) and the p-value of significance (p-value <0.05 -> significant at 5% level of falsely rejecting the null hypothesis of linear regression coefficient =0).

25

26

27



358

359 Extreme (RR10) and total precipitation RR show the following: a negative trend in the first decade of
360 the month turns in opposite to positive trends in the third (and second) month's decade, that indicate a
361 time-shift towards end-April -May of accumulated precipitation peak along April month. We note that
362 this feature of precipitation shift is present systematically in each model of the five-member CMIP5
363 ensemble (Karl et al. 2011). RR10 (and RR20, not shown) extremes enhance even more towards 2070.
364 Also, RR10 and RR show higher variability with significantly higher isolated extremes in the third
365 decade of the month in scenario compared to Hist. Extreme daily precipitation is, in most cases
366 detrimental for the crop, causing soil erosion and surface runoff after drought periods.

367

368

369 **b) Phenology and Yield projected changes for the control genotype**

370

371 Projected changes in phenology were simulated with the DSSAT forced by multi-model Hist and
372 climate scenarios RCP45 and RCP85, using first the control genotype G0 (Pioneer 375*) of the region.
373 The implemented system validation was done in Control simulations that used reanalysis climate data
374 from ERA5 (Simmons, 2021) over 1976-2005. These show a good time variability of the simulated
375 Yield against available measured values for the region, and that the modeling system is able to capture
376 years of high and low yield (Fig.5). The model set-up involved soil parameters calibration, that was
377 performed along sensitivity experiments for soil water and Nitrogen and Carbon organic content.

378



379

380

381 Fig. 5: Harvest simulated under twelve default management scenarios (Table 1, 3N) and measured (red
382 thick line), for the S-Romania. Blue box shows the Pearson correlation between treatments and
383 measured Harvest with statistical significance (***) $p=0.01$; **) $p=0.02$; *) $p=0.05$).

384

385

386

387 **b.1) Phenology dates - projected changes**

388

389 Ensemble model simulations over 30 year scenarios up to 2050, compared against historical runs (for
390 RCP 4.5 and RCP 8.5) indicate projected changes in the anthesis and maturity days in Fig. 6, for the
391 control genotype G0, fertilization 3N (Table 1, experiment E_3N_G0). These show that the anthesis
392 date is projected to occur earlier by up to ~6 days while maturity days come also earlier by up to about
393 10 days (ensemble mean, time mean), regardless of the planting date and the fertilization level. The two
394 shifts together lead to a shortening of the growing season by up to 10%. The average maturity date

28

29

30



395 may show small variations with the fertilization level, due to occurrence of slowed grain feeling (Fig.
396 6).

397

398

399

400

401

402

403

404

405

406

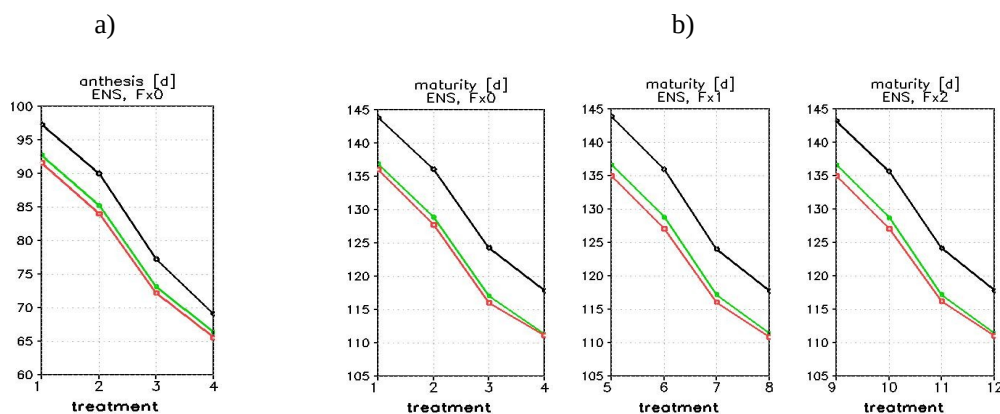
407

408

409

410

411



412 Fig.6: a) Anthesis dates ([dap], day after planting) simulated for the historical period (black), RCP45
413 scenario (green) and RCP85 scenario (red) for treatments 1 to 4; b) the same for the maturity date, for
414 treatments 1 to 12. On the Ox axis there are the treatments (1-12, Table 1, 3N, experiment E_3N_G0).

415

416

417 b.2) Yield - projected changes

418

419 Same multi-model simulations experiment E_3N_G0 show an overall decrease, in the ensemble mean,
420 of the yield in both climate scenarios, for all tested (Table 1) management scenarios with perturbed
421 sowing dates and fertilization levels (Fig. 7a,b,c).

422

423 This decrease was related to several factors: - a decrease in the accumulated rainfall in the growing
424 period (Fig. 8a,b,c) in scenarios compared to Hist in both climate scenarios and for all managements
425 scenarios; - a systematic earlier flowering date and date of reaching physiological maturity, the two
426 leading a shortening of the crop season (Fig. 6); - a decrease of fertilization efficiency with increasing
427 warming: the decrease in Harvest in scenario compared to Hist is higher for later sowing dates and for
428 higher emission in RCP8.5 than in RCP4.5 (Fig. 7c).

429

430 In the non-fertilized (Fig. 7a) case, we note is a Harvest increase with delaying sowing, for Hist and for
431 scenarios, indicating in the lack of nutrients, a stronger relation with precipitation: more accumulated
432 precipitation (Fig. 8a) for later dates (season's length increases for later sowing, for all treatments).
433 Also, RCP85 shows higher H values than RCP45 due to precipitation time shift (Fig. 4), more
434 appropriate for the plant development phase. This is no more valid when fertilization occurs (Harvest
435 decreases are obtained for later sowing dates in this case) pointing to nonlinear relation climate-
436 fertilization and to a decay of fertilization efficiency with warming.

437 The robustness of these is further analyzed in sensitivity simulations with enriched soil nutrients.

438

439

31

32

33



440 b.3) Sensitivity of changes to nutrients

441

442 In a second experiment we use the same fertilization levels but change in addition the initial soil
443 content in Carbon and Nitrogen (increased). The aim is to understand if less fertilization (less pollution)
444 could be compensated by better soil characteristics choice. Achieving best Harvest in warmer climate
445 versus actual climate enhancing the support towards a neutral climate, is a crucial point.

446 The sensitivity ensemble simulations increase soil Carbon and Nitrogen at the initial time by 20%, for
447 the same control genotype (Experiment E_1N_G0_soil+CN).

448

449

450

451

452

453

454

455

456

457

458

459

460

461

462

463

464

465

466

467

468

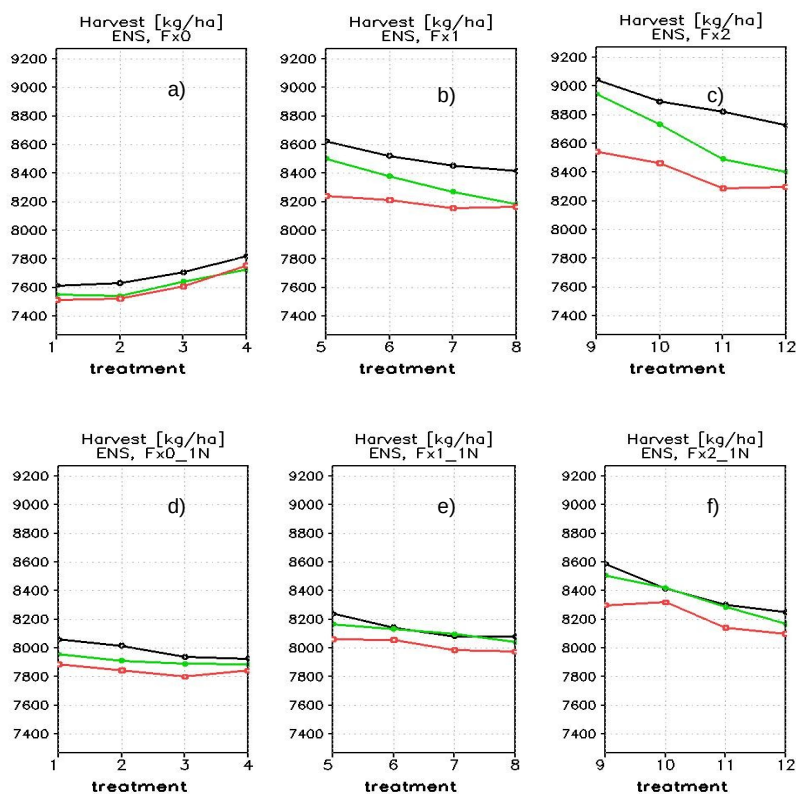
469

470

471

472

473



474 Fig. 7: Same as Fig. 6d, for Harvest [kg/ha] for experiment E_3N_G0 (top) and for experiment
475 E_1N_G0_soil+CN (bottom).

476

477

478 Experiment E_1N_G0_soil+CN compared to E_3N_G0 (Fig.7) shows that the Harvest is reduced by
479 only up to 7% for about 60% reduction in fertilization when the soil nutrients content is increased by
480 20%. In addition, we note two interesting features also for adaptation decisional support. One is that
481 there are still options even under warmer climate to overestimate the historical Harvest under
482 appropriate initial soil composition (e.g. in RCP45 TR6 and TR7, Fig. 7e) and even under RCP85
483 (TR10 and TR11, Fig.7f). The mechanism behind appears to be linked to richer soil (N, C) leading to a
484 slower maturity (Fig. 8b) with consequent more precipitation accumulated along the growing season

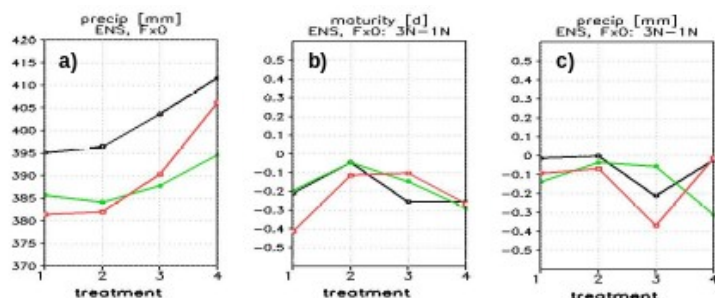
34

35

36



485 (Fig. 8c). This slower maturity is stronger for early sowing (Fig. 8b) hence better date option (Fig. 7d,
486 differences diminishing at later sowing due to precipitation shift).
487
488



489
490

491 Fig.8: a): Accumulated precipitation from the initial time of the simulation until the maturity date
492 ([mm]), for scenarios as in Fig.7, for E_3N_G0; in b) are shown differences [dap] in the maturity date
493 and in precipitation for (E_3N_G0) minus (E_1N_G0_soil+CN); c) same differences as in b) for the
494 precipitation accumulated along growing season ([mm]).
495

496

497 In summary for the control genotype, in both climate scenarios, and for all the management scenarios
498 tested for sowing-date and fertilization level but keeping the same genotype, it is projected a
499 shortening of the growing season (and earlier development phases) with mean decrease of the projected
500 yield. Meanwhile, it is shown that one can get comparable outcomes if astuciously using soil richness,
501 elongating the growing season, instead of enhancing fertilization levels and pollution.
502

503

504 c) Optimal genotype identification

505

506 The system was further developed to extend the management scenarios for multi-genotype simulations
507 and algorithms for optimal identification under each agro-climate scenario. Best options are searched
508 that lead to optimal (user-defined) yield: highest harvest, stable yield, less pollutant.

509

510 Two optimization methods are implemented: a discrete-value pure deterministic technique and a hybrid
511 optimization technique combining deterministic modeling with ML Genetic Algorithms for iterative
512 selection.

512

513 Deterministic method performs multiple simulations (and optimisation is part of the the post-
514 processing), for pre-established limits and discretisation intervals for each of the genotype parameters
515 considered (here six). Multi-model simulations in which each parameter is varied while the others have
516 fixed values are performed, resulting in a number of simulations depending on the discretisation. An
517 example for the criteria of “maximum yield” is illustrated in Fig.9a, for six genotype parameters: P1 the
518 thermal time from seedling emergence to the end of the juvenile phase; P2 a photoperiod-development
519 delay parameter; P3: the thermal time from silking to physiological maturity; P4 linked to maximum
520 kernels per plant, P5 linked to kernel filling rate and P6 the phyllochron interval), for Hist, RCP45 and
521 RCP85, each for the twelve default sowing date- fertilization treatments and each model of the

37
38
39



521 ensemble. We discuss here the results of genotype optimization (experiments E_1N_Gn+w) that are
522 based on the setup of E_1N_G0 but in which we increased the initial soil water content by 5% as
523 indicated by the projected maximum change over the pilot area (Fig. 1S, Suppl). Parameter P4 was kept
524 constant as having known impact.

525
526

527 **i) Optimal Harvest under climate change**

528

529 Fig. 9 shows, for the ordered genotype upon Harvest (H), a projected average decrease of the Harvest
530 (H) in maximum values' genotype-range range (top 2.5% cases), for RCP45 and emphasized also in
531 RCP85 for earlier sowing. This response is not systematic among models (Fig. 2S, Suppl). Among
532 models, we note a strong link between H differences and models' projected precipitation (a parameter
533 with high intra-model variability and regional-scale uncertainty) mainly for unfertilized case. In
534 opposite, the warming trend is a parameter in models' consensus for this region, leading to systematic
535 responses as earlier anthesis and maturity dates with a season shortening in RCP45 and even more in
536 RCP85 affecting mainly in the range of highest H (Fig. 3S, Suppl).

537 We further analyze robust features of the projected yield that are systematically seen among model-
538 simulations. Important climate-adaptation information appears from these diagrams.

539

540 One is the different response obtained for maximum H (GX) and for intermediate H (GI). Any
541 ("n") ordered simulations has a harvest, and a genotype associated, that we call "H-range" and
542 respectively "G-range" (of the top "n"-th value of H). We call GX the ranges of highest H values, GI of
543 intermediate H values and GN of lowest H values.

544 The large ensemble of genotype-treatment simulations indicate a decrease that is projected for the
545 highest yield (GX, Fig.9b) that is projected in RCP45 and RCP85 (except late sowing, low fertilization,
546 potentially linked to precipitation shift towards later in April mainly in RCP85). In opposite, a H
547 increase is projected for the intermediate yield genotype ranges (GI) for almost all treatments (Fig. 9c).
548 The explanation comes from the fact that we test a broad range of parameter P3 (the thermal interval to
549 maturity) and H increases significantly with P3 increase, in scenarios relative to Hist, a cause being the
550 fact that at highest values of P3 the plant maturity comes earlier in scenario compared to Hist with an
551 overall shortening of the season (with increasing P3, allowing stage accomplishment). These two
552 tendencies become systematic for all models in RCP85. Tendency towards H overestimations in
553 scenarios is not excluded neither for the Control genotype under conditions of higher soil water as it
554 was already noticed in Fig.7 e,f for the control Genotype. Here its G-parameters are located in the
555 intermediate range (400-1400) and have a central P3 value, but a lower initial soil moisture.
556 P3 value appears a key parameter on managing H. However care should be taken as extreme P3
557 increase leads to a too slow grain filling, and crop failure, more often in scenarios than in Hist (Fig.
558 3S), when P3 is above a threshold (that is P1 and P2 dependent, not shown).

559 The second feature is the fact that while for the highest H (GX) range it is systematic that earlier
560 sowing conditions are better options in E_1N_Gn+w (as P1 is small in maximal H), this is no more
561 valid for intermediate H genotype ranges (GI, Fig. 9a zooms, more days with precipitation improving
562 mainly the unfertilised cases). We note ranges with e.g. TR2 worse than TR3 (at GI ranges) and better
563 than TR1 (at GX ranges) mainly in RCP85. At mid-low H (ranges 1400-1890, GI, GN), there are

40
41
42



564 intervals of cross-parameter (sowing-fertilization) critical cases under unfertilized early sowing, rather
 565 than fertilized (top zoom in Fig. 9a, e.g. for RCP85).

566

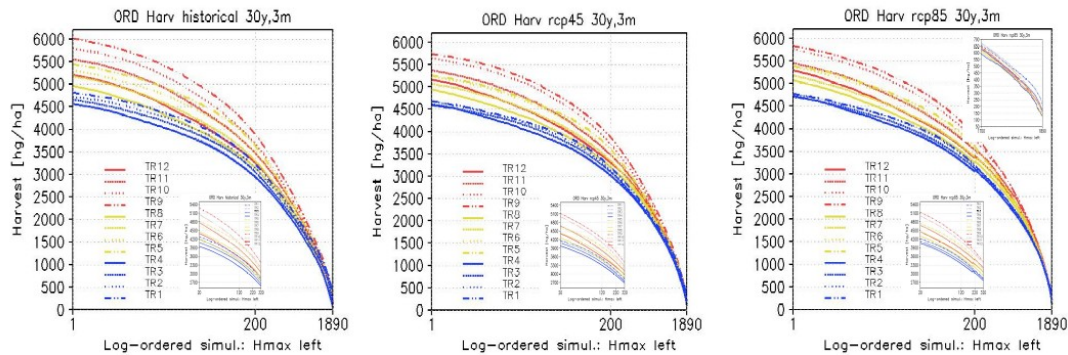
567 How one can use the PREPCLIM-v1 system output to assess a best management under climate
 568 scenarios? For a given genotype one can identify in these diagrams, either the optimal sowing-
 569 fertilization for a given scenario (on the vertical O_x =constant on Fig. 9a), or, for a given H one can
 570 identify the genotype ranges (per each sowing-fertilization) allowing this solution (line O_y =constant on
 571 Fig. 9a). These may propose variate options to improve yield, using the modeling system.

572

573 Third, we note a systematic narrowing of the spread among treatments (all models, all scenarios, as
 574 shown in Fig. 9a) all along genotype spectra (G-range belts), indicating a reduction of response options
 575 in future.

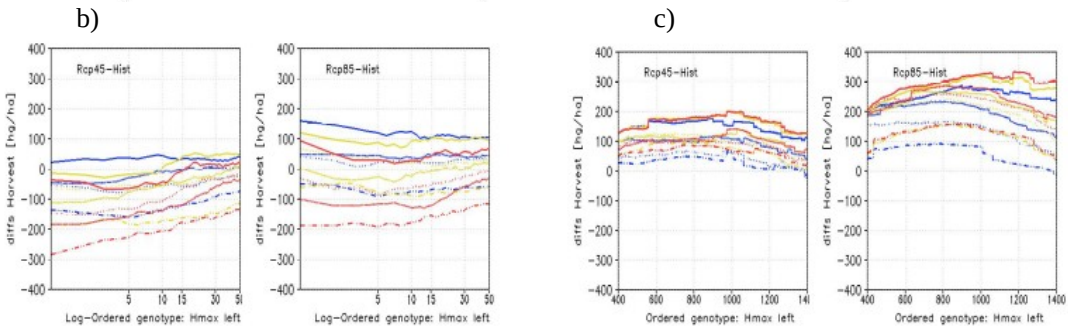
576

577 a)



578

579



580

581

582 Fig.9 a): Ordered simulation results for Harvest (O_y , model ensemble mean, time mean over 30 years).
 583 The simulations are for: Hist (left), Rcp45 (middle) and Rcp85 (right); a logarithmic scale was used
 584 for the simulations index in order to emphasize high H values. On O_x is the simulation rank (logarithmic
 585 scale) increasing for decreasing H (set-up E_{1N_Gn+w} with cross-genotype changes in six Pi
 586 parameters resulting 1890 experiments); each panel has a small zoom over intermediate H genotype
 587 ranges [20-320] at bottom and over [1700-1890] for RCP85, top corner; b) differences of H over two
 588 genotype range windows indicating a mean change for: the window of highest H in (b) ; c) same as b)
 589 for the window of intermediate H values. Colors in b) and c) have the same meaning as in a).

43

44

45



590

591 The third feature to be noticed is the role of the initial soil moisture. We note that the control genotype
592 in E_1N_G0+soil (Fig. 7d,e,f) falls in the intermediate H values of E_1N_Gn+w here (Fig. 9) with
593 higher yield in scenarios than Hist, feature already but marginally reached in Fig 7e,f, mainly due to
594 enhanced initial soil moisture in E_1N_G0_soil+w. In this regard, Fig.1Sa indicates a projected overall
595 decrease in soil moisture over the main agricultural area in the target region, with stronger decrease in
596 the Eastern and SE parts.

597

598

599 **ii) Optimal Genotype under climate change**

600

601 We saw a response of optimal H to the genotype choice in climate scenarios, and a different one for the
602 highest H (highest 0-2.5% H), intermediate (interval 21%-75% of genotype range) and then lowest H
603 values. For practical applications the crop projected response should be discriminated per genotype
604 parameter (P1-P6) to provide efficient support in adaptation decisions.

605 We analyze the role of each P1-P6 genotype sub-parameter related to crop performance under climate
606 scenarios versus Hist.

607

608 Management-genotype scenarios show that main drivers of increasing H in Hist runs are: decreasing P1
609 the thermal interval seedling-juvenile phase and decreasing the photoperiod delay parameter P2 (their
610 increases are associated with lower H). Contributions come then from a longer thermal time to maturity
611 (increasing P3), increasing the kernel-filling rate P5, and decreasing the phyllochron interval P6. The
612 slopes of Pi variation as a function of G-ranged index (the index increasing from maximal H to
613 minimal H) are positive for P1 and P2, negative for P3 and for P5 and P6 positive only in the GX range
614 of highest Harvest.

615 At lowest H we mention a particular sensitivity behavior of mainly P3 and P5 under increased
616 fertilization and sowing date. In this case, both small and high P values may lead to H decreases
617 (Fig.10a). This is related to critical situations of too slow grain filling that occur at high P3. We raise
618 warning for careful consideration when perturbing parameters as P3, P5 to perform genotype
619 adaptation, requiring additional modelling: finer discretisation of genotype parameters intervals, highly
620 accurate soil conditions set-up, close analysis of warming thresholds and phenology interactions
621 implied).

622

623 How one can use the PREPCLIM-v1 system output to assess a best genotype range under climate
624 scenarios? We compare scenarios against Hist first for the different Pi in Fig. 10. Simulations show for
625 all Pi a slope increase (Pi are functions of the G-ranged index) in the GX interval. Compensating the
626 slopes decrease in GI and GN (the variation limits for Pi being kept the same) in scenarios relative to
627 Hist. Relating these to H, we obtain estimates of projected impact of G-parameter perturbations, under
628 climate change.

629 For GX, the slope decrease found for positive slopes (P1,P2,P5,P6, Fig.10a) means that a G-
630 range in GX will be obtained up to higher Pi values than in Hist (Fig. 10b) hence an enlargement of
631 actually possible values (lower Pi values correspond to higher H in positive slopes). For GX, the slope
632 increase found for the negative slope of P3 means that higher H values than a given H-range here will
633 require higher P3 values (seen Fig 10b, as high values are giving best H in negative slopes), so
634 constraining its variation interval in GX to a narrower interval. This can be understood as a constraint

46

47

48



635 on using P3 for enhancing H and an enhanced efficiency on using P1,P2,P5,P6 options for enhancing H
636 under warmer climate, for maximal H (GX range).

637 For GI, a same analysis, links the slope increase for positive slopes (P1, P2, P5, P6, Fig. 10a) to
638 constraints on these parameters as options for increasing H, while the slope decrease of negative slope
639 for P3 represents an enhanced efficiency on using this parameter for improving H in the intermediate
640 range values.

641 For GN as discussed above, the response present bifurcations in the relation (Pi,H) and careful
642 simulations are required. These are however very important in the critical years, when yield is
643 estimated to be very low and we are searching for solutions. Note that over GN P6 has a third slope
644 change (otherwise main, non-bifurcated slopes and changes are as in GI), becoming positive (Fig.10a),
645 with enhanced efficiency.

646
647 We finally note the interesting aspect of differences between the two scenarios, in which important
648 changes of response (reversal) occur in P5 and P6 in RCP85 compared to RCP45, with consequent
649 impact on measure efficiency / constraint, that should be accounted for in adaptation.

650
651 In summary of the tis analysis, it is revealed that the main impact on H of genotype parameters'
652 changes are from P1, P2 and P3. It is shown that using shorter thermal time to flowering P1 values or
653 species with a shorter photoperiod-development delay P2 (for ensuring intermediate H-range values)
654 and higher P3 values (longer thermal time to maturity) for getting maximal H-range values are
655 constraints for Pi under warmer climate compared to Hist, emphasized for the pilot region.

656
657 Equally important, we note that changes in sign of responses (scenarios minus Hist) occur in Fig. 10b
658 in the GI range [400-1500], that is about the actual Control genotype range (Fig. 4S). This points
659 definitely to necessity for model simulations in order to identify which slight changes in Pi would lead
660 better or worse H in a warmer climate.

661
662 Regarding now the hybrid method deterministic-ML, this involves the same cross-simulations but this
663 time the selection of values for parameters is no more following a pre-defined discretisation and instead
664 it is a random picking up over a continuous interval of values and successively retrieving the best
665 generation, applying for optimization classic Genetic Algorithms methods in which selection of pairs is
666 based on the user-criteria (e.g. maximum yield, stable yield, etc.). Our results show that for the same
667 physical intervals of genotype parameters the ML hybrid technique only after 20 generations shows at
668 least 50% chances to get a better result than the deterministic model, while after 100 generations, it
669 already increases at 80% chances to get better results. A better result means here, identifying an
670 optimal configuration that has not been able to be emphasized by deterministic simulations.

671
672 In each of the two techniques used for optimal genotype identification, we note that in climate
673 scenarios versus historical climate, it is projected a significant narrowing of the management options
674 range leading, for a given genotype, to high yields (Fig. 8b), that is a severe warning for future decision
675 planning. Also there is a lower maxima potentially reachable under scenarios managements under
676 warmer climate (including genotype, sowing, fertilization).

677
678
679

49
50
51



680
 681
 682
 683
 684
 685
 686
 687
 688
 689
 690
 691
 692
 693
 694
 695
 696
 697
 698
 699
 700
 701
 702
 703
 704
 705
 706
 707

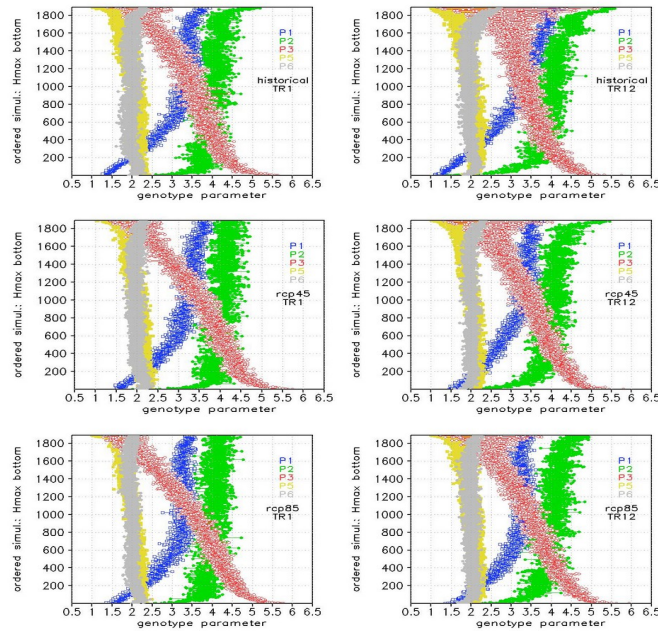


Fig.10a : Indices of the Genotype' six parameters (Ox) that correspond to Harvest ordered from max Harvest (Oy bottom) to min Harvest (Oy top). Here are 1890 genotypes (5x7x6x1x3x3 simulations with parameters, per model in [1,7]), shown as ensemble mean for two treatments (TR1 left column and TR12 right column). Indices are time-averaged (30 years) for simulations along Hist (top row), Rcp45 (middle row) and Rcp85 (bottom row) scenarios.

708
 709
 710

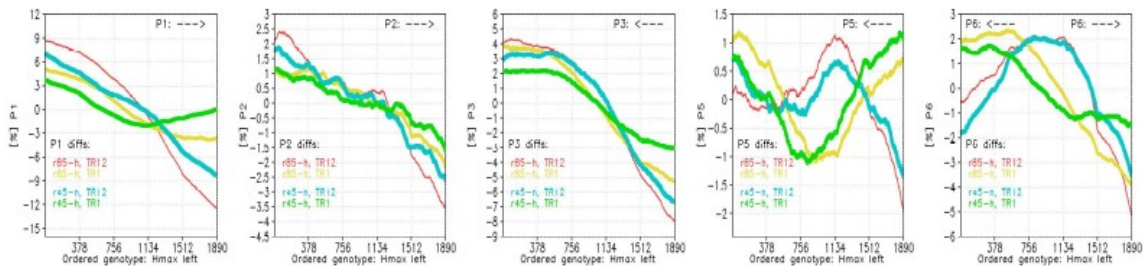


Fig. 10b: Percent changes in Genotype parameters Pi as a function of the ordered Harvest from highest (left, Ox) to lowest (right, Ox). Differences (running means over 378= $P_2 \cdot P_3 \cdot P_4 \cdot P_5 \cdot P_6$ values) are shown for TR1 (yellow for RCP45 minus Hist) and green (RCP45 minus Hist) and for TR12 (red (yellow for RCP85 minus Hist) and blue (for RCP45 minus Hist)). Differences in indices are expressed in percent relative to the parameter's range. Arrows indicate the (Pi,G-ranged index) overall linear trend from Fig.10a. (on Ox: the G-ranged index; on Oy the values of Pi).

52
 53
 54



717

718

719 The complex interactions for cross-parameters choice regarding sowing-fertilization-soil composition,
720 shown before, would make it difficult for assessing an optimal path, in the absence of a modeling
721 system. Even more, when it comes to choosing an optimal genotype with fixed or cross-optimal
722 sowing-fertilization-soil configuration the added value of such a modeling for optimum identification
723 becomes obvious and necessary, under warmer climate when traditional genotypes might no longer be
724 suitable.

725

726

727

728 **Discussions and Conclusions**

729

730 The main conclusion of this study is that an agroclimate real-time Interactive Service was developed
731 that goes beyond interrogation platforms for agro-climate information, stepping forwards and
732 performing in real-time, under user request, agro-management scenarios for the region. These allow
733 crop simulations for time-slice of interest, specified climate scenario, and user-specified management
734 scenarios.

735 A main novel feature of the system is the ability for identifying optimal management paths along cross-
736 cultivar management parameters and climate scenarios, as e.g. sowing date, genotype parameters,
737 amount and date of fertilization. The system provides solutions and uncertainty associated by using
738 multi-model ensemble for each agro-climate and management scenario. The optimisation criteria are
739 user-defined and can relate to high yield, stable yield, low pollution. The optimization module
740 implemented a hybrid deterministic and ML methodology. It performs multi-model simulations using
741 physical models of climate and plant phenology and optimisation is done either through simulating
742 discrete cross-parameters intervals pre-defined and optimisation post-processing, either using the
743 advantage of continuous parameter space investigation by using ML Genetic algorithms along multiple
744 model simulations. ML is spanning continuous parameter's space and interactively selecting along the
745 simulations the best fit parameters, allowing to identify unprecedented optimal configurations, not-
746 reachable under the discrete deterministic method.

747

748 The overall system output information is layered and accessed from two interfaces. One static, contains
749 high resolution agro-climate information (phenology, yield, extremes) at NUTS3 level that is useful for
750 user-analysis, management and adaptation and research. The second interface is interactive online
751 through which the system receives user requests and performs required simulations providing the
752 results. The user request refers to regional management scenarios or on optimal management
753 identification under climate change. These platforms are operational and were tested for two climate
754 scenarios RCP45 and RCP85 and twelve management scenarios (sowing dates and fertilization), for the
755 time-horizon up to 2050, with open-source code (EERIS platform). The results of these tests are
756 discussed here for the pilot region South Romania.

757

758 For the control genotype, in both climate scenarios it is projected a shortening of the growing season
759 (and an earlier shift of anthesis and maturity phases) and a mean decrease of the projected yield, for all
760 the management scenarios, sowing-date and fertilization level tested. We show that the decrease is also
761 linked to a lower efficiency of fertilization under warmer climate. Compared with the previous

55

56

57



762 observed unirrigated yields, here the shown reduction is significant (around 50%) in simulated yields of
763 rainfed corn cultivated in South-eastern Romania under the new climatic conditions.

764

765 However, we show that this response is highly sensitive to initial soil parameters as soil water content,
766 Nitrogen, Carbon. One could get an improved outcome if using richer soil (by 15%) but lower
767 fertilization (by 60%), elongating the growing season. This solution prevents a detrimental increase of
768 pollution that would otherwise enhance climate warming. It is shown the importance of precipitation
769 projections in relation with the sowing date: a time-shift towards end-April was identified in climate
770 scenarios for the region with an important link to planting date's Harvest.

771

772 The results for optimal genotype identification show, for the pilot area, under warmer climate two main
773 features. One is a mean decrease of maximal reachable H (in the genotype G-range of highest harvest
774 values) linked to a reduction of the agro-season length in the same genotype range (and earlier anthesis
775 and maturity dates). This response becomes systematic for all models in RCP85. Another is for the
776 genotypes range of intermediate H values, under climate scenarios, where rising tendencies are found.
777 These are linked on one hand to the broader range allowed for the P3 parameter (thermal time to
778 maturity), higher P3 values leading higher H-range even against season' length decrease as shown
779 further in the G-parameter analysis. To note here that caution is required and additional modeling of P3
780 extreme increases that give uncontrolled (bifurcation) of the H response as it leads, above a threshold
781 (P1 and P2 dependent) to crop failure due to a too slow grain filling, at a higher rate in scenarios than in
782 Hist. On the other hand, another contribution to higher intermediate-range harvest comes from the
783 mean precipitation decade-shift, mainly in RCP85 projections.

784 When discriminating the results upon genotype parameters we obtain that the main H changes are
785 linked to changes in P1 and P3 the thermal times to juvenil/ maturity phases. We show that there is a
786 stronger constraint to their decrease respectively increase.

787 Using shorter thermal time to flowering P1 values or species with a shorter photoperiod-development
788 delay P2 (for a same intermediate Harvest range) and longer thermal time to maturity P3 for maximal
789 H-range values are constraints emphasized for Pi under warmer climate compared to Hist.

790 These could be exploited in adaptation strategies for enhancing yield optimization in scenarios. We
791 showed that the actual Control genotype falls in the broader range of most sensitive H response to these
792 changes for the region.

793

794 It was shown that the optimisation search is improved by using a hybrid ML genetic algorithm method
795 coupled to the deterministic model-output, leading to detecting better optimal solutions. Of equal
796 perspective interest would be using the system for managing critical levels under periods of prolonged
797 or extreme drought, as emphasized in climate projections. As shown here, extreme events changes
798 under warmer climate (frost, precipitation shift, heat stress and soil moisture deficit, etc) are projected
799 to occur at different crop stages. In addition we showed that sink-source relationships (fertilization
800 efficiency - harvest, initial soil humidity) are projected to change, all leading to changes in yield
801 parameters. Hence, targeted understanding, validation and identification of optimal configurations
802 (genotype-management) for extreme cases or dynamics of their physical links, appropriate to alleviate
803 the impact, are a perspective of near-future exploitation of the system.

804

805 The main outcome of this work is the implementation and demonstration of the ability of deterministic
806 coupled modeling system combined with data-driven modeling for identifying optimal crop solutions.

58

59

60



807 This can be extended for other regions, scenarios, crops as a performant tool for adaptation support and
808 agro-climate research. Futures perspectives are opened to use the system for more complex issues as
809 rainfed yield level and stability in the new climatic conditions, where combination of cultivar
810 dependent coefficients that control the phenology of maize could help identify in the same way,
811 phenological evolutions that are more performant in certain patterns of water and heat stress
812 distribution along the year. Also, the improvement of the forecasts for the 6-12 months range may
813 increase chances to use this methods with weather prediction data in order to early select the most
814 suitable combination of hybrids for the current agro-season. Automatisation of these processes already
815 done, further supports extending the system towards a pilot regional agro-climate digital twin fed with
816 actualized data.

817

818

819 **Code and data availability:** The code is available in the Github repository at:
820 <https://github.com/pneague/Genetic-Algorithm-for-Corn-Genotype-Planting-Date-Optimization> under
821 a BSD 2-Clause Simplified License.

822

823 **Author contribution:** MC: model implementation, code for optimal adaptation tool, pre and post-
824 processing, model simulations, results analysis, development of the User-Platform, paper writing; LC:
825 DSSAT model set-up, simulations, results analysis, paper review; PN: ML method implementation and
826 runs, results analysis, paper writing; AD: model validation; VA: development of the Info-Platform; ZC
827 and AI: platforms upload and update; AP: agro-meteorological station data providing; GC: DSSAT
828 model input for the target region.

829

830

831 **Competing interests:** The contact author has declared that none of the authors has any competing
832 interests

833 **Disclaimer**

834 Any use of trade, firm, or product names is for descriptive purposes only and does not imply
835 endorsement by the U.S. Government.

836 Publisher's note: Copernicus Publications remains neutral with regard to jurisdictional claims made in
837 the text, published maps, institutional affiliations, or any other geographical representation in this
838 paper. While Copernicus Publications makes every effort to include appropriate place names, the final
839 responsibility lies with the authors.

840

841 **Acknowledgments:** The authors are grateful to UEFISCDI who provided the financial support of this
842 work under the Project Grant PREPCLIM-PN-III-P2-2.1-PED-2019-5302.

843

844 **References:**

61

62

63



- 845 Malhi, G.S., Kaur, M. and Kaushik, P., 2021. Impact of climate change on agriculture and its
846 mitigation strategies: A review. *Sustainability*, 13(3), p.1318.
- 847 Eyring, V., Mishra, V., Griffith, G.P., Chen, L., Keenan, T., Turetsky, M.R., Brown, S., Jotzo, F.,
848 Moore, F.C. and Van der Linden, S., 2021. Reflections and projections on a decade of climate science.
849 *Nature Climate Change*, 11(4), pp.279-285
- 850 Wheeler T, Joachim von Braun. Climate change impacts on global food security. *Science*. 2013 Aug
851 2;341(6145):508-13. doi: 10.1126/science.1239402. DOI: 10.1126/science.1239402
- 852 Godfray, H., Charles J., et al. (2010) Food Security: The Challenge of Feeding 9 Billion People.
853 *Science*, 327, 812-818.
- 854 World Development Report 2008: Agriculture for Development, World Bank
- 855 Vaclav Smil Vaclav Population and Development Review , pp. 605-643 (39 pages) Published By:
856 Wiley
- 857 Villalobos, Francisco & Pérez-Priego, Oscar & Testi, Luca & Morales, Alejandro & Orgaz, Francisco.
858 (2012). Effects of water supply on carbon and water exchange of olive trees. *European Journal of*
859 *Agronomy*. 40. 1-7. 10.1016/j.eja.2012.02.004.
- 860 Rocuzzo G, Zanotelli D, Allegra M et al (2012) Assessing nutrient uptake by field-grown orange
861 trees. *Eur J Agron* 41:73–80. doi:10.1016/j.eja.2012.03.011
- 862 Semenov, Mikhail & Stratonovitch, Pierre. (2015). Adapting wheat ideotypes for climate change:
863 Accounting for uncertainties in CMIP5 climate projections. *Climate Research*. 65. 10.3354/cr01297.
- 864 Mitchell R.J, Paul E. Bellamy, Alice Broome, Chris J. Ellis, Richard L. Hewison, Glenn R. Iason, Nick
865 A. Littlewood, Scott Newey, Gabor Pozsgai, Duncan Ray, Jenni A. Stockan, Victoria Stokes, Andy F.
866 S. Taylor . Cumulative impact assessments of multiple host species loss from plant diseases show
867 disproportionate reductions in associated biodiversity. *Journal of ecology*.
868 <https://doi.org/10.1111/1365-2745.13798>
- 869 Espadafor M., Francisco Orgaz, Luca Testi, Ignacio Jesús Lorite, Victoria González-Dugo, Elías
870 Fereres, Responses of transpiration and transpiration efficiency of almond trees to moderate water
871 deficits, *Scientia Horticulturae*, Volume 225, 2017, Pages 6-14, ISSN
872 0304-4238, <https://doi.org/10.1016/j.scienta.2017.06.028>.
- 873 Dainelli Riccardo & Calmanti, Sandro & Pasqui, Massimiliano & Rocchi, Leandro & Di Giuseppe,
874 Edmondo & Monotti, Chiara & Quaresima, Sara & Matese, Alessandro & Di Gennaro, Salvatore &
875 Toscano, Piero. (2022). Moving climate seasonal forecasts information from useful to usable for early
876 within-season predictions of durum wheat yield. *Climate Services*. 28. 100324.
877 10.1016/j.cliser.2022.100324.



- 878 Abhik Patra, Vinod Kumar Sharma, Dhruva Jyoti Nath, Asik Dutta, Tapan Jyoti Purakayastha,
879 Sarvendra Kumar, Mandira Barman, Kapil Atmaram Chobhe, Chaitanya Prasad Nath & Chiranjeev
880 Kumawat (2022): Long-term impact of integrated nutrient management on sustainable yield index of
881 rice and soil quality under acidic inceptisol, Archives of Agronomy and Soil Science, DOI:
882 10.1080/03650340.2022.2056597
- 883 Tao Fulu, Zhao Zhang, Jiyuan Liu, Masayuki Yokozawa,Modelling the impacts of weather and climate
884 variability on crop productivity over a large area: A new super-ensemble-based probabilistic projection,
885 Agricultural and Forest Meteorology,Volume 149, Issue 8,2009,Pages 1266-1278,ISSN 0168-
886 1923,https://doi.org/10.1016/j.agrformet.2009.02.015.
- 887 Ganguly Sangram, Mark A. Friedl, Bin Tan, Xiaoyang Zhang, Manish Verma,Land surface phenology
888 from MODIS: Characterization of the Collection 5 global land cover dynamics product,Remote
889 Sensing of Environment,Volume 114, Issue 8,2010,Pages 1805-1816,ISSN
890 0034-4257,https://doi.org/10.1016/j.rse.2010.04.005.
- 891 Asseng, Senthold & Ewert, Frank & Martre, Pierre & Rötter, Reimund P. & Lobell, D. & Cammarano,
892 Davide & Kimball, B. & others, and. (2015). Rising temperatures reduce global wheat production.
893 Nature Climate Change. 5.
- 894 Kholová J., Milan Oldřich Urban, James Cock, Jairo Arcos, Elizabeth Arnaud, Destan Aytekin, Vania
895 Azevedo, Andrew P Barnes, Salvatore Ceccarelli, Paul Chavarriaga, Joshua N Cobb, David Connor,
896 Cooper Mark, Peter Craufurd, Daniel Debouck, Robert Fungo, Stefania Grando, Graeme L Hammer,
897 Carlos E Jara, Charlie Messina, Gloria Mosquera, Eileen Nchanji, Eng Hwa Ng, Steven Prager,
898 Sindhujan Sankaran, Michael Selvaraj, François Tardieu, Philip Thornton, Sandra P Valdes-Gutierrez,
899 Jacob van Etten, Peter Wenzl, Yunbi Xu, In pursuit of a better world: crop improvement and the
900 CGIAR, Journal of Experimental Botany, Volume 72, Issue 14, 10 July 2021, Pages 5158–5179,
901 https://doi.org/10.1093/jxb/erab226
- 902 Yi Chen, Fulu Tao,Potential of remote sensing data-crop model assimilation and seasonal weather
903 forecasts for early-season crop yield forecasting over a large area,Field Crops Research,Volume
904 276,2022,108398,ISSN 0378-4290,https://doi.org/10.1016/j.fcr.2021.108398.
- 905 Schauburger, B., J. Jägermeyr, and C. Gornott, 2020: A systematic review of local to regional yield
906 forecasting approaches and frequently used data resources. Eur. J. Agron., 120, 126153,
907 doi:10.1016/j.eja.2020.126153.
- 908 Baez-Gonzalez, Alma Delia & Kiniry, James & Maas, Stephan & L, M. & C, J. & Mendoza, Jose &
909 Richardson, Clarence & Salinas, & Manjarrez, Juan. (2005). Large-Area Maize Yield Forecasting
910 Using Leaf Area Index Based Yield Model. Agronomy Journal. 97. 10.2134/agronj2005.0418.



- 911 Jin X., Jin Y., Zhai J., Fu D., Mao X. Identification and prediction of crop Waterlogging Risk Areas
912 under the impact of climate change. *Water*, 14 (2022), pp. 1-21, 10.3390/w14121956
- 913 Meehl G.A., T.F. Stocker, W.D. Collins, A.J. Gaye, J.M. Gregory, A. Kitoh, R. Knutti, J.M. Murphy,
914 A. Noda, S.C.B. Raper, J.G. Watterson, A.J. Weaver, Z. Zhao. *Global Climate Projections*. S.
915 Solomon, D. Qin, M. Manning, Z. Chen, M. Marquis, K.B. Averyt, M. Tignor, H.L. Miller (Eds.),
916 Cambridge University Press, Cambridge, U.K. and New York, NY (2007)
- 917 Rosenzweig, C., J.W. Jones, J.L. Hatfield, A.C. Ruane, K.J. Boote, P. Thorburn, J.M. Antle, G.C.
918 Nelson, C. Porter, S. Janssen, S. Asseng, B. Basso, F. Ewert, D. Wallach, G. Baigorria, and J.M.
919 Winter, 2013: The Agricultural Model Intercomparison and Improvement Project (AgMIP): Protocols
920 and pilot studies. *Agric. Forest Meteorol.*, 170, 166-182, doi:10.1016/j.agrformet.2012.09.011.
- 921 Basso, B., Shuai, G., Zhang, J. et al. Yield stability analysis reveals sources of large-scale nitrogen loss
922 from the US Midwest. *Sci Rep* 9, 5774 (2019). <https://doi.org/10.1038/s41598-019-42271-1>
- 923 Chapagain Ranju, Remenyi Tomas A., Huth Neil, Mohammed Caroline L., Ojeda Jonathan
924 J. Investigating the effects of APSIM model configuration on model outputs across different
925 environments. *Frontiers in Agronomy*.
926 <https://www.frontiersin.org/articles/10.3389/fagro.2023.1213074>.
927 DOI=10.3389/fagro.2023.1213074,ISSN=2673-3218
- 928 Bernardo, R. *Breeding for Quantitative Traits in Plants*. 9780972072403.
929 <https://books.google.ro/books?id=3T2FQgAACAAJ> 2002. Stemma Press
- 930 Hoogenboom G., Porter, Cheryl & Boote, Kenneth & Shelia, Vakhtang & Wilkens, Paul & Singh,
931 Upendra & White, Jeffrey & Asseng, Senthold & Lizaso, Jon & Moreno Cadena, Patricia & Pavan,
932 Willingthon & Ogoshi, Richard & Hunt, L. & Tsuji, Gordon & Jones, James. (2019). The DSSAT crop
933 modeling ecosystem. 10.19103/AS.2019.0061.10.
934
- 935 Jones, J., Hoogenboom, G., Porter, C., Boote, K., Batchelor, W., Hunt, L. and Ritchie, J., 2003. The
936 DSSAT cropping system model *European Journal of Agronomy*. 18:235-265
937 ([https://doi.org/10.1016/S1161-0301\(02\)00107-7](https://doi.org/10.1016/S1161-0301(02)00107-7))
- 938 Cooper Mark, Carlos D Messina, *Breeding crops for drought-affected environments and improved*
939 *climate resilience*, *The Plant Cell*, Volume 35, Issue 1, January 2023, Pages 162–186,
940 <https://doi.org/10.1093/plcell/koac321>
- 941 Qiao, Linyi & Xiaojun, Zhang & Li, Xin & Yang, Zujun & Li, Rui & Jia, Juqing & Yan, Liuling &
942 Chang, Zhijian. (2022). Genetic incorporation of genes for the optimal plant architecture in common
943 wheat. *Molecular Breeding*. 42. 10.1007/s11032-022-01336-2



- 944 Ming Li, Yonglu Tang, Chaosu Li, Xiaoli Wu, Xiong Tao, Miao Liu, Climate warming causes changes
945 in wheat phenological development that benefit yield in the Sichuan Basin of China,
946 European Journal of Agronomy, Volume 139, 2022, 126574, ISSN
947 1161-0301, <https://doi.org/10.1016/j.eja.2022.126574>.
- 948 Morell F-J, Haishun S. Yang, Kenneth G. Cassman, Justin Van Wart, Roger W. Elmore, Mark Licht,
949 Jeffrey A. Coulter, Ignacio A. Ciampitti, Cameron M. Pittelkow, Sylvie M. Brouder, Peter Thomison,
950 Joe Lauer, Christopher Graham, Raymond Massey, Patricio Grassini, Can crop simulation models be
951 used to predict local to regional maize yields and total production in the U.S. Corn Belt?, Field Crops
952 Research, Volume 192, 2016, Pages 1-12, ISSN 0378-4290, <https://doi.org/10.1016/j.fcr.2016.04.004>.
- 953 Morales, Alejandro & Villalobos, Francisco. (2023). Using machine learning for crop yield prediction
954 in the past or the future. *Frontiers in plant science*. 14. 1128388. [10.3389/fpls.2023.1128388](https://doi.org/10.3389/fpls.2023.1128388).
- 955 van Ittersum Martin K. , Kenneth G. Cassman, Patricio Grassini, Joost Wolf, Pablo Tittonell, Zvi
956 Hochman, Yield gap analysis with local to global relevance—A review, *Field Crops Research*, Volume
957 143, 2013, Pages 4-17, ISSN 0378-4290, <https://doi.org/10.1016/j.fcr.2012.09.009>.
- 958 Boogaard Hendrik , Joost Wolf, Iwan Supit, Stefan Niemeyer, Martin van Ittersum, A regional
959 implementation of WOFOST for calculating yield gaps of autumn-sown wheat across the European
960 Union, *Field Crops Research*, Volume 143, 2013, Pages 130-142, ISSN
961 0378-4290, <https://doi.org/10.1016/j.fcr.2012.11.005>. [https://www.sciencedirect.com/topics/agricultural-](https://www.sciencedirect.com/topics/agricultural-and-biological-sciences/crop-simulation-model)
962 [and-biological-sciences/crop-simulation-model](https://www.sciencedirect.com/topics/agricultural-and-biological-sciences/crop-simulation-model)
- 963 Xie, W., Zhu, A., Ali, T. et al. Crop switching can enhance environmental sustainability and farmer
964 incomes in China. *Nature* 616, 300–305 (2023). <https://doi.org/10.1038/s41586-023-05799-x>
- 965 Asseng A, Y. Zhu, B. Basso, T. Wilson, D. Cammarano, Simulation Modeling: Applications in
966 Cropping Systems <https://doi.org/10.1016/B978-0-444-52512-3.00233-3a>, *Encyclopedia of Agriculture*
967 *and Food Systems* 2014, Pages 102-112
- 968 Zhuang, H., Zhang, Z., Cheng, F., (...), Xu, J., Tao, F., Integrating data assimilation, crop model, and
969 machine learning for winter wheat yield forecasting in the North China Plain , 2024. *Agricultural and*
970 *Forest Meteorology*
- 971 Wimalasiri, E.M., Sirishantha, D., Karunadhipathi, U.L., (...), Muttill, N., Rathnayake, U. Climate
972 Change and Soil Dynamics: A Crop Modelling Approach 2023 *Soil Systems*
- 973 Rezaei, E.E., Webber, H., Asseng, S., (...), Martre, P., MacCarthy, D.S. Climate change impacts on
974 crop yields 2023, *Nature Reviews Earth and Environment*



- 975 Mamassi, A., Balaghi, R., Devkota, K.P., (...), El-Gharous, M., Tychon, B. Modeling genotype ×
976 environment × management interactions for a sustainable intensification under rainfed wheat cropping
977 system in Morocco 2023 Agriculture and Food Security
- 978 Alsafadi, K., Bi, S., Abdo, H.G., (...), Chandran, M.A.S., Mohammed, S. Modeling the impacts of
979 projected climate change on wheat crop suitability in semi-arid regions using the AHP-based weighted
980 climatic suitability index and CMIP6 2023 Geoscience Letters
- 981 Paudel Dilli, Hendrik Boogaard, Allard de Wit, Marijn van der Velde, Martin Claverie, Luigi Nisini,
982 Sander Janssen, Sjoukje Osinga, Ioannis N. Athanasiadis, Machine learning for regional crop yield
983 forecasting in Europe, Field Crops Research, Volume 276, 2022, 108377, ISSN 0378-4290,
984 <https://doi.org/10.1016/j.fcr.2021.108377>.
- 985 Peleman J-D, Jeroen Rouppe van der Voort, Breeding by Design, Trends in Plant Science, Volume 8,
986 Issue 7, 2003, Pages 330-334, ISSN 1360-1385, [https://doi.org/10.1016/S1360-1385\(03\)00134-1](https://doi.org/10.1016/S1360-1385(03)00134-1).
- 987 Pfeiffer, Wolfgang & McClafferty, Bonnie. (2007). HarvestPlus: Breeding Crops for Better Nutrition.
988 Crop Science - CROP SCI. 47. 10.2135/cropsci2007.09.0020IPBS.
- 989 Bai, Y., Yue, W. and Ding, C., 2021. Optimize the Irrigation and Fertilizer Schedules by Combining
990 DSSAT and GA.
- 991 Wang, Y., Jiang, K., Shen, H., Wang, N., Liu, R., Wu, J. and Ma, X., 2023. Decision-making method
992 for maize irrigation in supplementary irrigation areas based on the DSSAT model and a genetic
993 algorithm. Agricultural Water Management, 280, p.108231.
- 994 Shaw, T.A., Miyawaki, O. Fast upper-level jet stream winds get faster under climate change. *Nat.*
995 *Clim. Chang.* 14, 61–67 (2024). <https://doi.org/10.1038/s41558-023-01884-1>
- 996 Lelieveld, J., Hadjinicolaou, P., Kostopoulou, E. *et al.* Climate change and impacts in the Eastern
997 Mediterranean and the Middle East. *Climatic Change* **114**, 667–687 (2012).
998 <https://doi.org/10.1007/s10584-012-0418-4>
- 999 Arnell, N.W., Freeman, A. The effect of climate change on agro-climatic indicators in the UK. *Climatic*
1000 *Change* 165, 40 (2021). <https://doi.org/10.1007/s10584-021-03054-8>.
- 1001 Trnka M et al (2014) Adverse weather conditions for European wheat production will become more
1002 frequent with climate change. *Nat Clim Chang* 4:637–643
- 1003 Hatfield JL et al (2020) Indicators of climate change in agricultural systems. *Clim Chang* 163:1719–
1004 1732
- 1005 Selvaraju R et al (2011) Climate science in support of sustainable agriculture and food security. *Clim*
1006 *Res* 47:95–110



- 1007 Stehr N, von Storch H (2009) Climate and society: climate as resource, climate as risk. World
1008 Scientific Pub Co Inc, Hackensack
- 1009 R. Benestad, E. Buonomo, J.M. Gutiérrez, A. Haensler, B. Hennemuth, T. Illy, D. Jacob, E.K. Thiel, E.
1010 Katragkou, S. Kotlarski, G. Nikulin, J. Otto, D. Wretched, T. Remke, K. Sieck, S. Sobolowski, P.
1011 Szabó, G. Szépszó, C. Teichmann, R. Vautard, T. Weber, *Guidance for EURO-CORDEX climate*
1012 *projections data use, Version 1.1*, 2021
- 1013 Simmons, A. , *The ERA-Interim archive Version 2.0, ERA Report Series*, 2021
- 1014 Karl E. Taylor, Ronald J. Stouffer, Gerald A. Meehl, *A summary of the CMIP5 Experiment Design*,
1015 2011
- 1016 Adams, R. M., Hurd, B. H., Lenhart, S., & Leary, N. (1998). Effects of global climate change on
1017 agriculture: an interpretative review. *Climate Research*, 11(1), 19–30.
1018 <http://www.jstor.org/stable/24865973>
- 1019 MKee, T.B.; Doesken, N.J.; Kleist, J. *The Relationship of Drought Frequency and Duration to Time*
1020 *Scales*. In Proceedings of the Eighth Conference on Applied Climatology, Anaheim, CA, USA, 17–22
1021 January 1993; pp. 179–184.
- 1022 Marcinkowski, P., Piniewski, M. (2018): *Effect of climate change on sowing and harvest dates of*
1023 *spring barley and maize in Poland*. - *International Agrophysics*, 32, 2, 265-
1024 271.<https://doi.org/10.1515/intag-2017-0015>
- 1025 Antonio Berti, Carmelo Maucieri, Alessandra Bonamano Maurizio Borin, *Short-term climate change*
1026 *effects on maize phenological phases in northeast Italy*, Nov 2019, Italian Journal of Agronomy DOI:
1027 [10.4081/ija.2019.1362](https://doi.org/10.4081/ija.2019.1362)
- 1028 Andrej Ceglar, Matteo Zampieri, Nube Gonzalez-Reviriego, Philippe Ciais, Bernhard Schauburger and
1029 Marijn Van der Velde, *Time-varying impact of climate on maize and wheat yields in France since*
1030 *1900*, *Environmental Research Letters*, Volume 15, Number
1031 [9https://doi.org/10.1088/1748-9326/aba1be](https://doi.org/10.1088/1748-9326/aba1be)
- 1032 Webber et al. 2020, *Pan-European multi-crop model ensemble simulations of wheat and grain maize*
1033 *under climate change scenarios*, Open Data Journal for Agricultural Research, vol. 6, p. 21-27
- 1034 Webber, H., Ewert, F., Olesen, J.E., Müller, C., Fronzek, S., Ruane, A.C., Bourgault, M., Martre, P.,
1035 Ababaei, B., Bindi, M., Ferrise, R., Finger, R., Fodor, N., Gabaldón-Leal, C., Gaiser, T., Jabloun, M.,
1036 Kersebaum, K.-C., Lizaso, J. I., Lorite, I.J., Manceau, L., Moriondo, M., Nendel, C., Rodríguez, A.,
1037 Ruiz-Ramos, M., Semenov, M.A., Siebert, S., Stella, T., Stratonovitch, P., Trombi, G. and Wallach, D.,
1038 2018a. “*Diverging importance of drought stress for maize and winter wheat in Europe*”. *Nature*
1039 *Communications* 9(1): 1-11. doi: 10.1038/s41467-018-06525-2.



1040 Jian-zhai Wu, Jing ZHANG, Zhang-ming GE, Li-wei XING, Shu-qing HAN, Chen SHEN, Fan-tao
1041 KONG, *Impact of climate change on maize yield in China from 1979 to 2016*, Journal of Integrative
1042 Agriculture, Volume 20, Issue 1, 2021, Pages 289-299, ISSN 2095-3119,
1043 [https://doi.org/10.1016/S2095-3119\(20\)63244-0](https://doi.org/10.1016/S2095-3119(20)63244-0).

1044

1045

1046

1047 **Annex 1: Data and Methods**

1048

1049 Schema of steps in work-flow of ML algorithms for optimal genotype identification:

- 1050 ● Start with 10 randomly chosen solutions within the bounds of P1-P6;
1051 ● Calculate the mean and std of harvest of each solution for the 30 years 1976-2005;
1052 ● Calculate fitness = (Mean of harvest) – (Standard-deviation of Harvest/4);
1053 ● Randomly choose 4 pairs of ‘parents’, with the probability being chosen weighted by the
1054 fitness;
1055 ● For each pair of parents A and B, create identical children ‘a’ and ‘b’ to the parents, then choose
1056 a random number of P’s to be subjected to crossover, called x;
1057 ● For each child, modify P_x as follows:
1058 ○ $P_{xa} = \text{round}(B * P_{xa} + (1 - B) * P_{xb})$
1059 ○ $P_{xb} = \text{round}(1 - B) * P_{xa} + B * P_{xb}$

1060 Where P_{xa} is the value of the x parameter of child a (initially identical to that of parent A), and
1061 B is the blending factor, set in this paper to 0.75. This technique is called blending and it
1062 generates offspring chromosomes that inherit real-valued traits from both parents while
1063 exploring the search space between the parents’ positions. The blending crossover promotes a
1064 smoother and more gradual search for optimal solutions in continuous domains;

- 1065 ● Then take each child, and with a probability of 0.5 perform a mutation on one of its
1066 chromosomes. This means setting one of the P’s to a random value between its allowed
1067 minimum and maximum;
1068 ● At this point the children have been fully constructed. Discard the 8 parents with the lowest
1069 fitness and substitute them with the children;
1070 ● Repeat.

1071

1072

1073